Biophysical Chemistry 144 (2009) 53–61

Contents lists available at ScienceDirect

Biophysical Chemistry

journal homepage: http://www.elsevier.com/locate/biophyschem

A molecular dynamics model of the Bt toxin Cyt1A and its validation by resonance energy transfer

Xiaochuan Li [a,1], Kerrick J. Nevels [a,2], Zygmunt Gryczynski [b], Ignacy Gryczynski [b], Marianne Pusztai-Carey [c], Dexuan Xie [d,*], Peter Butko [e,*]

[a] Department of Chemistry and Biochemistry, University of Southern Mississippi, Hattiesburg, MS 39406, USA
[b] Department of Molecular Biology and Immunology, University of North Texas Health Science Center, Fort Worth, TX 76107, USA
[c] Department of Biochemistry, Case Western Reserve University, Cleveland, OH 44106, USA
[d] Department of Mathematical Sciences, University of Wisconsin, Milwaukee, WI 53201, USA
[e] Department of Pharmaceutical Sciences, University of Maryland School of Pharmacy, 20 N. Pine Street, PH 515, Baltimore, MD 21201, USA

ARTICLE INFO

Article history:
Received 9 March 2009
Received in revised form 26 May 2009
Accepted 9 June 2009
Available online 16 June 2009

Keywords:
Bacillus thuringiensis toxin
CHARMM
NAMD
Mutation
Computer simulation
Resonance energy transfer

ABSTRACT

Cyt1A is a cytolytic toxin from *Bacillus thuringiensis* var. *israelensis*. A computer model of the toxin in solution was generated and validated by resonance energy transfer (RET). The average distance between the two tryptophans (residues 158 and 161) and the fluorescently labeled cysteine 190 was 2.16 nm, which closely matched the distance predicted in computer simulations, 2.2 nm. The simulation results were able to explain two previous experimental observations: (i) amino-acid sequences of all Cyt toxins contain four blocks of highly conserved residues; and (ii) several single-point mutations drastically abrogated Cyt1A's toxicity. Selective randomization of atomic coordinates in the computer model revealed that the conserved blocks are important for proper folding and stability of the toxin molecule. Replacing lysine 225 with alanine, a mutation that renders the toxin inactive, was shown to result in breaking the hydrogen bonds between K225 and V126, L123, and Y189. Calculated Helmholtz free energy difference of the inactive mutation K225A was higher by 12 kcal/mol and 5 kcal/mol than the values for the benign mutations K118A and K198A, respectively, which indicates that the K225A mutant is significantly destabilized. The normal-mode and principal-component analyses revealed that in the wild-type Cyt1A the region around the residue K225 is quite stationary, due to the hydrogen-bond network around K225. In contrast, pronounced twisting and stretching were observed in the mutant K225A, and the region around the residue K225 becomes unstable. Our results indicate that conformational differences in this mutant spread far away from the site of the mutation, suggesting that the mutant is inactivated due to an overall change in conformation and diminished stability rather than due to a localized alteration of a "binding" or "active" site.

1. Introduction

The δ endotoxins of *Bacillus thuringiensis* (also called Bt toxins, from the abbreviated name of the bacterial source) are divided into two families: the insect-specific Cry (for crystal) toxins and Cyt (for cytolytic) toxins, which are generally cytolytic in vitro [1]. The Cyt proteins are toxic in vivo to the larvae of members of the order Diptera, which includes mosquitoes and black flies. Hence, the Cyt toxins have been used for decades in commercial insecticidal preparations, despite our incomplete understanding of their mechanism of action at the molecular level. It was clear from the early experiments with the toxin Cyt1Aa1 (formerly known as CytA and abbreviated throughout this paper as Cyt1A) and artificial lipid membranes that the cytolytic effect of the toxin does not require binding to a membrane receptor, but rather is mediated by direct binding to the lipid [2–4]. It is less clear how the toxin manages to lyse the cell or lipid vesicle. One hypothesis postulates oligomeric channels or pores formed by the toxin [4,5], while another invokes a less-specific detergent-like mechanism of the toxin's action [6]. Preliminary attempts to visualize Cyt1A pores directly by atomic force microscopy have been presented in 2001 [7], but other evidence suggests that the membrane-bound toxin has an open irregular conformation similar to molten globule [6,8], which is difficult to reconcile with the notion of a well-defined protein-lined pore. A molten globule is very dynamic, with secondary structural elements largely retained, but with no tertiary structure. It is therefore possible that the conformation of the Cyt1A toxin in or on the membrane will never be experimentally determined, simply because there is none: the membrane-bound Cyt1A may assume a continuum of more or less disordered conformations. If that is indeed

* Corresponding authors. Butko, Tel.: +1 410 706 8521; fax: +1 410 706 0346. Xie, Tel.: +1 414 229 3528.
E-mail addresses: dxie@uwm.edu (D. Xie), pbutko@rx.umaryland.edu (P. Butko).
[1] Present address: Department of Physiology and Biophysics, Boston University, 715 Albany Street, Boston, MA 02118, USA.
[2] Present address: Department of Pharmaceutical Sciences, University of Maryland School of Pharmacy, 20 N. Pine Street, Baltimore, MD 21201, USA.

0301-4622/$ – see front matter © 2009 Elsevier B.V. All rights reserved.
doi:10.1016/j.bpc.2009.06.005

the case, experimental techniques may yield some kind of ensemble-average information, but not a single, true structure. As we have already argued elsewhere [9], molecular dynamics (MD) simulations [10,11] is a good tool to approach this in the absence of experimental data.

In a previous paper [12] we have laid the groundwork: we generated the solution conformation of Cyt1A by homology modeling based on the experimentally determined structure of the related toxin Cyt2Aa1 [13]; refined it by energy minimization; and carried out several short-term (sub-nanosecond) MD simulations. One result of that work was the identification of regions on the toxin's surface that manifest increased conformational flexibility and thus are likely to participate in the initial binding to the lipid membrane. In the present paper we validate the model by fluorescence spectroscopy and employ it to study the significance of the four conserved blocks in amino-acid sequences of all Cyt toxins and the possible structural impact of a single-point mutation that is known to abrogate Cyt1A's toxicity in vivo.

The amino-acid sequence alignment of Cyt toxins revealed four conserved blocks of similarity. Using numbering of amino acids for Cyt1A, they are found in: (i) α helix A (residues 51–68, consensus sequence YILQAIMLANAFQNALVP); (ii) the loop and the short β strand after helix D (residues 146–161, consensus sequence TFTNLNTQKNEAWIFW); (iii) β strands 5 and 6 with the interconnecting loop (residues 169–196, consensus sequence TNYTYNVLFAIQNAQTGGVMYCVPVGFE); and (iv) α helix E (which was prior to the current simulation tentatively assigned the β strand character and labeled β6a [9]) with the following loop (residues 207–217, consensus sequence LFFTIQDSASY [9]). The four conserved block regions are colored green, blue, cyan, and red, respectively, in Fig. 1. To study their significance, we used "selective randomization" of atomic coordinates: the atoms in the residues either within the conserved blocks or outside the blocks were shifted in random directions by some random distances. After potential energy minimization, energies of the two randomized systems were compared with that of the native protein, which allowed us to suggest the possible role of the conserved blocks.

Ward et al. [14] carried out an extensive mutagenesis study of Cyt1A, where they replaced one by one numerous, mostly charged, amino acids with alanine. Lipid-binding assays and in vivo toxicity assays revealed that some mutations were inconsequential, but some abrogated the toxicity to various degrees. It might be tentatively assumed that the mutated residues are important for electrostatic interactions with the lipid head groups. However, it is equally possible that the mutated residues do not directly bind to the lipid, but rather provide stability to the native, active conformation of the toxin. We addressed this issue by modeling selected mutations in the toxin molecule to see whether in solution, i.e., in the absence of the lipid membrane, the mutants exhibit altered conformations and/or different behavior. To that aim we used molecular dynamics simulation, normal-mode and principal-component analyses and free-energy difference calculations.

2. Materials and methods

2.1. Computer simulations

The full-length Cyt1A has 249 residues with 3846 atoms and a molecular weight of 27334.1 Da. Amongst the 249 residues, 13 are positively charged and 20 are negatively charged, giving the molecule an estimated net charge of −7*e* at neutral pH. The Cyt1A and mutant conformations were generated and analyzed with Visual Molecular Dynamics (VMD) [15]. For some residues in Cyt1A there are no experimental structural data (residues 1–16, 47–48, 86–92). Since the N-terminal portion of the toxin is cleaved in proteolytic activation of Cyt1A (either in the insect's gut or in the laboratory), the first 19 residues were not included in the MD simulations, free-energy difference calculation, and normal-mode analysis except in the four conserved blocks minimization study. Atomic coordinates of the remaining missing residues were generated by CHARMM and were manually adjusted to fit the appropriate secondary structures as deduced from homology modeling based on Cyt2Aa1 crystal structure [13]. The mutated Cyt1A (K225A) was created in VMD by a script. Both the wild-type Cyt1A and the K225A mutant had almost the same energy (−3230 kcal/mol and −3169 kcal/mol, respectively).

Two molecular dynamics software packages, CHARMM [16,17], versions c29b2 or c34b2, and NAMD [18,19], version 2.5, were used in this work. We implemented our MD simulations in two schemes: implicit and explicit solvent environments. Wild-type Cyt1A, K225A, K118A, and K198A were dissolved in a water box of size $75.54 \times 67.11 \times 63.86$ Å^3 respectively and all of them were simulated by NAMD for over 10 ns. The

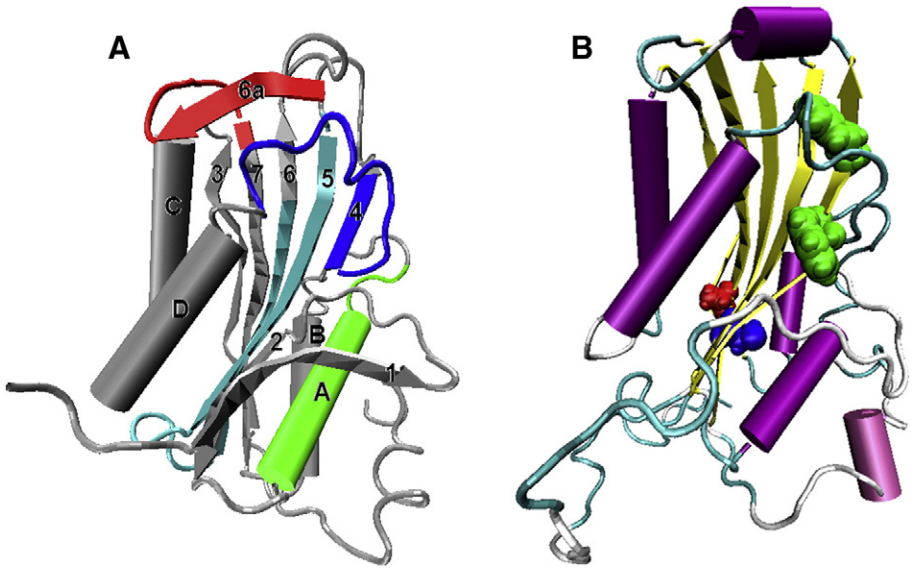

Fig. 1. (A) The initial conformation of Cyt1A rendered by VMD [18,19]. The four conserved blocks are colored green (α helix A), blue (the short β strand 4 and the loop connecting it to the helix D), cyan (β strands 5 and 6), and red (the helix E, previously thought to be strand 6a, and the loop connecting it to the strand 7). (B) The mutant K225A, in which lysine 225 was mutated to alanine, shown in red. Two tryptophans, W158 and W161, are showed in green and cysteine 190 is colored in blue. Structure of Cyt1A, taken from [9], was produced by SpdbViewer [34], while that of the mutant was drawn by VMD according to STRIDE algorithm [35].

study on the conserved blocks of Cyt1A through energy minimization (version c29b2); calculations of free energy difference between the wild type and the K225A, K118A, and K198A mutants; and normal mode analysis on wild-type Cyt1A and K225A were carried out with CHARMM version c34b2.

Energy minimization was performed using the residue topology file "top_all22_prot.inp" and the parameter file "par_all22_prot.inp" from CHARMM version c29b2. The atom-pair distance cutoff radius was set to 9 Å. Two widely used minimization algorithms, the steepest descent (SD) and the adopted-basis Newton–Raphson (ABNR), were employed with the maximum allowable iteration steps 40,000 for SD and 20,000 for the subsequent ABNR. The minimization process was terminated when either the gradient root-mean-square (GRMS) value of 0.0001 kcal/(mol Å) or the maximum number of steps was reached.

To investigate the importance of the four conserved blocks in Cyt1A, and also to make sure that our simulation results did not depend on the particular initial conformation, energy minimizations were carried out with slightly different initial conformations that were generated by the formula

$$\vec{r}_{\text{new}} = \vec{r}_{\text{old}} + \text{rand}(0:1) \times f \tag{1}$$

where $\vec{r}$ is the position vector of an atom (in Å), f is a factor that governs the magnitude of the position change, and rand(0:1) is a random vector of three random numbers between 0 and 1. The sign of factor f is determined by a fourth random number between 0 and 1: when the fourth random number <0.5, the sign of f is negative, otherwise it is positive. In order to study the influence of the initial conformation on MD results, all atoms in the molecule were randomly shifted from their equilibrium positions using Eq. (1) with $f = 1$ Å, and the effect on the energy minimum and the final MD conformation was determined. The same equation with a much larger value of f (= 20 Å) was used to study the effect of "selective randomization" on the energy of the molecule. Here only selected regions of the toxin molecule underwent randomization of atomic coordinates and thus significance of the particular regions for overall stability of the molecule could be assessed.

Free energy difference and normal mode analysis were carried out in implicit solvent scheme of GBSW (Generalized Born with a simple Switching) [20,21] with CHARMM version c34b2. GBSW provides the electrostatic and non-polar solvation energies and forces for the CHARMM force field so that individual water molecules do not have to appear in the computations. It utilizes a simple smoothing function at the dielectric boundary. The parameter SW was set to 0.3; the non-polar surface tension coefficient sigma was set to 0.005 kcal/mol Å^2; the number of angular integration points was set to 50 and the salt concentration to 0.15 M. We used nonbonded interactions ctonnb 16 ctofnb 20 cutnb 24, the CHARMM residue topology file "top_all27_prot_na.rtf", and the parameter file "par_all27_prot_na.prm", along with "toppar_all27_na_nad_ppi.str". The atom-pair distance cutoff radius was set to 9 Å.

The Helmholtz free energy difference ($\Delta\Delta A$) is defined as the difference between the free energy changes in the native and mutated protein, and theoretically it should equal to the experimentally determined free energy difference. The development of thermodynamic perturbation techniques has been described in a number of papers [22–25], therefore here just briefly. The free energy difference ΔA between states A and B can be calculated as:

$$\Delta A = A_B - A_A = -kT \ln \langle e^{-\Delta H/kT} \rangle_A \tag{2}$$

where $\Delta H = H_B - H_A$ and $\langle \rangle_A$ represents ensemble average over configurations sampled in the system in state A. CHARMM divides the system's atoms into four groups: the environment, the colo, the reactant, and the product atoms. The reactant and product atoms are those that are actually being changed; the colo atoms are those in which only the charge changes in going from reactant to product; the environment atoms comprise the rest of the system. The free energy change upon mutation can be computed by perturbation theory with the intermediate Hamiltonian $H(\lambda)$ given by

$$H(\lambda) = H_o + \lambda H_B + (1 - \lambda) H_A, \tag{3}$$

where λ is a coupling parameter with limiting values 0 for the wild type and 1 for the mutant, and H_o, H_A, and H_B are the "environment", "reactant", and "product" parts of the Hamiltonian. Eq. (2) then acquires the form

$$\Delta A = A_B - A_A = \sum_{\lambda=0}^{1} -kT \ln \langle e^{-\Delta H'/kT} \rangle_\lambda, \tag{4}$$

where $\Delta H' = H_{\lambda + d\lambda} - H_\lambda$. In this manner, free energy difference is calculated through many small windows, each with a sufficiently small change in l to allow for an accurate free energy calculation.

Normal mode analysis is routinely used to study harmonic vibrations of proteins, which in turn provide information about fundamental collective movements in the protein. A normal mode analysis was performed in an attempt to investigate the Cyt1A's functional behavior. Harmonic vibrations of atomic bonds were calculated, and the mass-weighted second derivative matrix was diagonalized to obtain the vibration frequencies. The analysis was limited to the lowest frequencies of normal mode, which represent superimposed collective vibrations that may be related to protein functions. A CHARMM utility was used, with Parameter set 19/22 and the GBSW force field.

Principal component analysis yields a basis set from which the average structure, with its dynamics, is constructed via linear combination. This method greatly reduces the dimensionality of the conformation space by limiting the analysis to only the most significant components of macromolecular dynamics.

In order to speed up the computation of MD simulations in explicit solvent, we employed NAMD, a parallel MD package designed for high-performance simulations of large biomolecular systems on parallel computers. The CHARMM27 force field for proteins and lipids [17] and the TIP3P model for water [26] were used.

VMD plugin scripts "autopsf" and "solvate" were used to create the required psf and pdb files. The toxin was solvated in silico with a 10 Å thick layer of water, with water molecules within 0.8 Å of the protein surface deleted. The protein–water complex of Cyt1A and its mutant K225A had dimensions of $75.54 \times 67.11 \times 63.86$ Å^3 with 29,400 and 29,391 water molecules, respectively. Aspartate, glutamate, lysine and arginine residues were assumed charged throughout the protein. A cutoff of 12 Å (the switching function starting at 10 Å) for van der Waals interactions was assumed, along with the periodic boundary condition. The latter [27] eliminated the boundary problem and also made the simulation of bulk water more manageable. The Particle Mesh Ewald (PME) method [28] with the rigid bond constraint turned on was used to compute long-range electrostatic forces. Density of the grid points for PME was at least 1/Å^3. After energy minimization, molecular dynamics simulation with 2-fs time steps was performed on protein–water complex for 2 ns at a constant temperature (300 K), controlled by Langevin Dynamics with a 2-ps^{-1} damping coefficient, and pressure (1 atm), controlled by Nose–Hoover and Langevin piston with a 100-fs decay period and a 50-fs damping time. The average conformations of Cyt1A and the mutant were obtained by averaging the last 500 frames because the system may not have reached the complete equilibrium. In order to visualize the toxin's conformation changes during MD, the average conformations at 0.5 ns, 1 ns, 1.5 ns, and 2 ns were calculated by averaging frames 225–275, 475–525, 725–775, and 950–1000, respectively. Similar MD runs with random seeds or different schemes were performed three times. All the numerical

simulations were carried out on the SGI Origin 2000 with 16 R12000 400 MHz processors at the University of Wisconsin-Milwaukee.

2.2. Experimental

The fluorescence probe 5-((((2-iodoacetyl)amino)ethyl)amino) naphthalene-1-sulfonic acid (1,5-IAEDANS) was from Molecular Probes (Eugene, OR) and N, N-dimethylformamide from Fisher Scientific (Pittsburgh, PA). All buffers and salts were from Sigma-Aldrich (St. Louis, MO), VWR (Atlanta, GA), or Fisher Scientific. Cyt1A was purified from cultures of *B. thuringiensis* var. *israelensis* as described before [29] and was fluorescently labeled by a straightforward procedure [30]. Cyt1A was dissolved in 0.1 M NH_4HCO_3, pH 8.5 to give a concentration of 0.2 mM. 1,5-IAEDANS was dissolved in N,N-dimethylformamide (DMF), pH>6, to give a concentration of 226 mM. A 50-fold molar excess of IAEDANS and 1 mM EDTA were added, and the solution was incubated for 2 h at 37 °C, after which the free probe was separated from the conjugate by size exclusion chromatography on a PD-10 column (GE Healthcare, Piscataway, NJ). The column was equilibrated with 25 ml of 0.1 M NH_4HCO_3, pH 8.5, and the labeled protein was eluted with the same buffer and collected in three fractions. Stoichiometry of labeling was determined by absorption spectroscopy on a Jasco V-530 UV-Vis spectrophotometer with the values of molar extinction coefficients 5700 M^{-1} cm^{-1} and 20,500 M^{-1} cm^{-1} for IAEDANS and Cyt1A, respectively, at the wavelengths of their respective absorption maxima, 336 and 280 nm. The toxin/dye molar ratio was 1:1.4 and the labeled toxin was 100% active in a red-blood-cell hemolysis assay.

For RET, steady-state fluorescence spectra were recorded with an ISS K2 spectrofluorometer (Champaign, IL). Spectra of labeled and unlabeled Cyt1A in NH_4HCO_3, pH 8.5, at a final concentration of 0.5 μM in a 3 mm × 3 mm quartz cell were collected. Fluorescence of IAEDANS was corrected for the non-negligible direct excitation of IAEDANS by the tryptophan-exciting light (280 nm) with the help of a factor found from the comparison of free IAEDANS fluorescence excited at 280 nm and 336 nm. RET efficiency E was calculated as $E = A_A(\lambda_D)/A_D(\lambda_D)[(I_{AD}(\lambda_D)/I_A(\lambda_D)) - 1]$, where λ_D is the wavelength of the absorption maximum of the donor, $A_A(\lambda_D)$ and $A_D(\lambda_D)$ are the acceptor and donor absorbances, respectively, at λ_D, and $I_{AD}(\lambda_D)$ and $I_A(\lambda_D)$ are the intensities of the acceptor emission at λ_D in the presence and absence of the donor, respectively [30]. Fluorescence lifetime of IAEDANS-labeled Cyt1A was determined using the PicoQuant Fluotime 200 time-resolved spectrometer (Berlin, Germany) with a pulsed 285 nm LED, having a resolving power of 100 ps. The sample in a 3 mm × 3 mm quartz cell contained 4 μM labeled Cyt1A. It was excited at 285 nm and the emission was measured at 344 nm through a 320 nm long pass filter. RET efficiency was calculated as $E = 1 - (\tau_{DA}/\tau_D)$, where τ_{DA} is the lifetime of the donor in the presence of acceptor and τ_D is the lifetime of the donor in the absence of the acceptor [30].

The distance between the fluorescence donor (tryptophan) and acceptor (IAEDANS) was calculated from the experimentally determined efficiency E as

$$R = R_0[(1-E)/E]^{1/6}, \quad (5)$$

where R_0 is the Forster radius, the distance at which $E = 1/2$. The value of R_0 was taken as 21.7 Å and the orientation factor κ^2 was implicitly assumed to be 2/3 [30].

3. Results and discussion

3.1. The initial conformation effects and selective randomization of atomic coordinates

To study the effects of initial conformation on MD simulation, we generated several initial conformations by using Eq. (1) and performed energy minimization. Same minimization scheme as we described early was applied on all conformations. The initial values of total energy E and GRMS were either infinity or a very large positive number, due to the randomized positions of atoms. But they were quickly reduced by SD iterations and the subsequent ABNR iterations until the termination rule, GRMS of less than 0.0001 or iteration number exceeding the maximum, was satisfied. In the results shown in Table 1, structures labeled R1 had $f = 1$ Å, which means that the positions of atoms were altered only slightly. This method was used to generate different initial conformations in our simulations. The label R2 indicates that $f = 20$ Å, which introduced a very significant disorder in the randomized regions of the protein. The same initial structure was used in generating all the conformations in Table 1. The first row of Table 1 lists the related minimization results. In the table, conformational energy ("Conf") is the sum of the bond-stretching, bond-bending, bond-torsion and improper energies; "Nonbond" energy includes van der Waals and Coulomb energies. The "Total" energy is the sum of "Conf" and "Nonbond", i.e., the total energy of the molecule. "Block", "non-block", and "side chains" denote those regions of Cyt1A whose atoms were randomized. Here "block" means that coordinates of the atoms in the conserved blocks of amino acids were randomly altered, whereas "non-block" means the opposite (i.e., the atoms in the blocks were kept in their equilibrium positions, while the coordinates of the rest of the atoms were randomized), and "side chains" means randomization in the amino-acid side chains but not of the peptide backbone. The values of minimum energy for the slightly perturbed conformations, labeled R1, are all close to each other. The perturbations were too small to yield any new insight. When the value of the parameter f was increased to 20 Å, perturbations were larger and, not surprisingly, pronounced changes in minimum energy were observed. Indeed, with this procedure, atoms might be randomly pulled out far beyond the surface of the molecule and the molecule itself might cease to exist in physical space. While it might be questioned whether sampling of physically unrealistic portions of the energy landscape has any bearing on the molecule's stability, one observation is inescapable: there is a considerable difference between two structures with reciprocal regions of randomization, "block" vs. "non-block". The structure with randomized non-block residues had the minimum energy just 670 kcal/mol above the energy of the initial native conformation. On the other hand, randomization of the block residues yielded an energy more than 4000 kcal/mol higher, despite the fact that the number of randomized atoms was less than half of those in the "non-block" randomization. In other words, Cyt1A is much more impervious to gross alterations outside the four conserved blocks than inside the blocks. This clearly indicates the importance of the conserved blocks for maintaining or attaining the proper native

Table 1
Effect of selective atomic randomization on the calculated energy minima.

Conformation	Number of randomized atoms	Conf	Nonbond	Total
		Energy [kcal/mol]		
Initial	0	2422	−5826	−3404
R1	3846	2510	−5940	−3430
R1 Non-block	2692	2437	−5799	−3362
R1 Block	1154	2422	−5869	−3446
R2 Non-block	2692	3288	−6021	−2733
R2 Block	1154	5538	−4689	849
R2 Side chains	3099	6113	−4659	1459

The R1-labeled conformations were only slightly modified, with the randomization factor $f = 1$ Å (see text), whereas the label R2 indicates more disorganized conformations, with $f = 20$ Å. Conformational energy "Conf" is the sum of the bond-stretching, bond-bending, bond-torsion and improper energies; "Nonbond" energy includes van der Waals and Coulomb energies. "Block", "non-block", and "side chains" denote regions of Cyt1A whose atomic coordinates were randomized: "block" refers to the conserved blocks in the amino-acid sequences of all Cyt toxins and "side chains" means that all atoms in the amino-acid side chains, but not those in the backbone, were randomized. The calculations were performed with CHARMM.

conformation of the toxin molecule. Interestingly, when all the side-chain atoms (i.e., 3 times more atoms than in the "blocks") were randomized, while the atoms of the peptide backbone were kept in their equilibrium positions, energy increased by only 600 kcal/mol. This again points to the paramount importance of the conserved block regions, which are responsible for the proper backbone conformation and for overall stability of the toxin molecule.

3.2. Validation of the model

The best way to validate a computer model of a macromolecule is to compare it with the experimentally determined structure. Up to date, the only known structure of a Cyt toxin remains that of the toxin Cyt2A, obtained by Li et al. [13]. But since that structure was the point of departure in creating our model, comparing the former to the latter would be a vicious circle. A suitable alternative is to measure an intramolecular distance (or even better — a set of distances) between specific points in the protein and compare the experimental data with the model. Fortuitously, Cyt1A contains a single cysteine residue, C190, which is readily amenable to fluorescence labeling, and two tryptophans, only 2 amino acids apart, on the short strand β4. Labeling the cysteine with the thiol-reactive fluorescence probe IAEDANS, which can act as a fluorescence energy acceptor for tryptophan, enabled us to estimate the distance between the cysteine and the tryptophans by RET.

Fig. 2 shows fluorescence spectrum of the IAEDANS-labeled Cyt1A excited at 280 nm. The fluorescence of IAEDANS, clearly visible at 473 nm, demonstrates energy transfer between the tryptophan donors and IAEDANS acceptor. Efficiency of the energy transfer, determined from the decrease of fluorescence lifetime of tryptophan in the labeled toxin (Fig. 3), was used to calculate the distance between the donors and the acceptor. The wild-type unlabeled Cyt1A molecule exhibited two fluorescence lifetimes of tryptophan, with the amplitude-weighted average of 4.4 ± 0.1 ns. The decay (the red line in Fig. 3) was well approximated by a two-exponential model with the lifetimes 2.3 and 5.3 ns and respective relative amplitudes of 0.31 and 0.69. The goodness of fit ($\chi^2 = 1.05$) did not improve significantly with the addition of a third component. When IAEDANS was covalently linked to C190, a third lifetime component was needed to obtain a good fit (the green line in Fig. 3), with the lifetimes 0.7, 2.3, and 5.2 ns and amplitudes 0.39, 0.45, and 0.16, respectively. The main point is

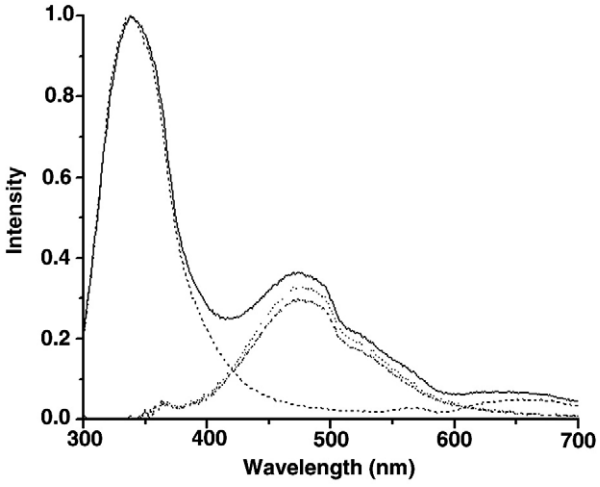

Fig. 2. RET from tryptophan to IAEDANS in Cyt1A. The solid line (—) represents IAEDANS-labeled Cyt1A excited at 280 nm. The dashed line (– – –) represents native Cyt1A excited at 280 nm. The dotted line (· · · ·) represents spectrum of IAEDANS fluorescence after subtracting the tryptophan fluorescence (solid line). The dash–dot (–·–·–) line represents fluorescence of IAEDANS due to energy transfer; it was obtained by subtracting direct excitation of IAEDANS with the 280-nm light from the dotted-line spectrum.

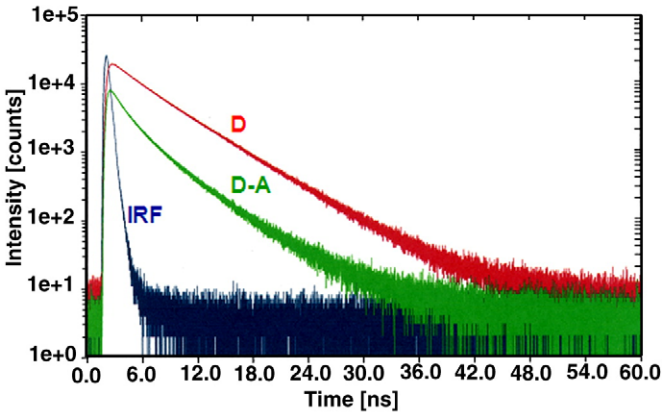

Fig. 3. Fluorescence intensity decays of the tryptophan emission from Cyt1A in the absence (red, D) and presence of IAEDANS acceptor (green, D-A), which was covalently linked to cysteine 190. The excitation flash is labeled IRF. (For interpretation of the references to color in this figure legend, the reader is referred to the web version of this article.)

that the amplitude-weighted average lifetime value decreased to 2.1 ± 0.1 ns, which signifies a 52% efficiency of RET. Further evaluation of these data is complicated by the fact that the single RET acceptor–IAEDANS–accepts energy from two donors in the molecule of Cyt1A — W158 and W161. The classical mathematical formalism of RET was developed for the case of single donor–acceptor pairs [31,32]. The problem of immobilized (i.e., non-diffusible) multiple donors/acceptors in complex geometries is encountered quite often in practice, but it has received little attention of theorists. Only recently numerical methods and computer simulations started to be employed in addressing the issue [33]. While efficiency of energy transfer is more-or-less directly measured in the experiment, the donor/acceptor distance is calculated from the RET data and its interpretation is contingent on factors such as the number of donors/acceptors and their mutual distances and orientations. Of course, one can always calculate a distance from any set of RET data, but, as in our case, the problem is what distance is actually calculated: Is it the distance from the cysteine to the nearest tryptophan or to the center of gravity of the two tryptophans or to some weighted average of the tryptophans' positions? The simplest of all the simplifying assumptions is that the measured RET efficiency can be subject to the classical formalism to calculate the distance between the acceptor and the midpoint between the two donor tryptophans, which is equivalent to saying that each of the two tryptophans contributes the same energy to the acceptor. This approach is simple, but unlikely to be true in general. Since efficiency of RET is a steep function of distance, efficiency of transfer from the more distant donor might be significantly lower than that from the nearer one, assuming the same rotational mobility of the two. Hence another simplifying assumption is possible, namely, that all energy is only transferred from the nearest donor, as the more distant donors would contribute progressively smaller fractions of energy. This also may not always be true, since transfer efficiency depends not only on distance, but also on the mutual orientation of the donor and acceptor. When the lifetime data were treated with the classical formalism for RET (which in our case means the assumption of equal energy transfer from the two tryptophans and essentially treating the latter as a single energy donor located midway between W158 and 161), an efficiency of 0.52 implied the distance 2.2 ± 0.1 nm (the error was calculated from the experimental uncertainty in lifetime determination). This was compared with the following distances extracted from the model: 1.80 nm for C190-W158, 2.54 nm for C190-W161, and the average ± range 2.2 ± 0.4 nm. Bearing in mind the above-mentioned interpretation difficulties, the average distance in the computer model, 2.2 nm, matches the value extracted from the experimental data. We conclude that, with the

caveats discussed above, the data are in accord with the model. The agreement between the theoretical and experimental values also supports the notion that the two tryptophans probably donate energy to the IAEDANS acceptor in equal, or sufficiently similar, proportions. Had that not been the case, the experimental value would be closer to either of the two values of the distance between C190 and the respective tryptophan (1.80 nm or 2.54 nm). Further validation of the model will come from future measurements of additional distances in single-tryptophan forms of Cyt1a, which are presently being constructed in our laboratory.

3.3. Free energy differences between the wild-type and mutated Cyt1A

When compared with the wild-type Cyt1A or the active mutants K118A and K198, the inactive mutant K225A consistently showed higher values of RMSD (Table 2), indicating differences in conformation. By using the previously described approach, free energy differences between the mutants and the wild type were calculated, as listed in Table 3. The enthalpy and entropy differences were calculated with the CHARMM TSM (Thermodynamic Simulation Method) module, using a tripeptide AKA as a reference, which showed the following values of changes in free energy ($\Delta A = -51$ kcal/mol), enthalpy ($\Delta H = -66$ kcal/mol) and entropy ($\Delta S = -0.05$ cal/(mol K)) upon mutating the central lysine to alanine. From Table 3 we can see that K225A is the least stable amongst the three mutants (with ($\Delta\Delta A = 28$ kcal/mol). Note that the enthalpy difference of K225A is highly positive, undoubtedly due to the removal of charge on the lysine and the subsequent abrogation of electrostatic stabilization.

To confirm our conclusions, we built another reference structure using the all amino-acid sequence and internal coordinates (IC) of Cyt1A by CHARMM. Even though the numbers were slightly different (not shown), K225A was again found to have the highest free energy difference, confirming that the mutant K225A is the least stable molecule of the three.

3.4. Normal-mode and principal-component analyses of the wild-type Cyt1A and mutant K225A

In the first nonzero normal mode of the wild-type Cyt1A, which has a frequency of 5.04 cm^{-1}, the β strand 1 and the C-terminus loop undergo cooperative motion. This contrasts with the first nonzero normal mode, at 5.82 cm^{-1}, of the mutant K225A, which behaved quite differently: in particular, two domains twisted around each other. In the next few normal modes, the wild-type Cyt1A exhibited two distinct domains, too. The upper domain includes α helices C and D, along with the β sheets, and the lower one consists of α helices A and B, and their respective loops. The fulcrum that connects the two domains lies along the horizontal line near the residue 225 (see Quicktime movies in Supplemental Material). The data indicate that Cyt1A has two relatively mobile domains that can move around the immobile center around K225. Importantly, motions of the two domains are completely different in the first 8 non-zero normal modes of the wild-type Cyt1A and the mutant K225A. We hypothesize that the mutation K225A disrupts the protein's stability and alters the fundamental modes of intramolecular motions (twisting, stretching, etc.), thus hindering the toxin's activity. Indeed, the second and higher normal modes in the wild type and the mutant K225A give support to this notion. At frequencies 6.18 cm^{-1} and 6.85 cm^{-1}, β strand 7 in K225A exhibited a twisting motion that did not appear in any of the normal modes in the wild-type Cyt1A. Because of the anchoring effect of the K225 side chain, at the frequency of 9.72 cm^{-1}, α helix C and β strand 7 move in synchrony in the wild-type Cyt1A. Quicktime movies of selected fundamental motions in the wild-type Cyt1A and mutant K225A can be viewed in Supplementary Material.

Results of principal component analysis essentially corroborated those of normal mode analysis. In particular, the first principal component at 9.15 cm^{-1}, which accounts for 19% of variance, was also prominent in normal mode analysis (mode #8): it describes a synchronous motion of α helix C and β sheet 7. These results confirmed those of our previous study [12] in that the most flexible regions of the toxin molecule are helices A and B and β sheet 1 at the bottom of the molecule and helix E and the loops on the top. Differences in dynamics between the wild type and the mutant K225A were also well exemplified in results of principal component analysis: while first four components account for 47% of variance in the wild type, they only account for 36% in the mutant. When we restricted principal component analysis only to the area surrounding K225, that is, amino acid residues 100 to 150 and 180 to 230 the motional differences between the wild type and the mutant, observed in normal mode analysis, became even more obvious: superimposed first 24 components showed only moderate and correlated motions in wild-type Cyt1A, whereas motions in the mutant were uncoordinated and long-ranged. The motions are captured in two Quicktime movies (cyt1a_pca and mutant_pca) in Supplementary Material.

3.5. NAMD simulation of the wild-type and mutated Cyt1A

Since our future goal is to model the interaction of Cyt1A with the lipid membrane, a system much more complex than a simple aqueous solution, we decided to use the parallel molecular dynamics program NAMD [18,19], which significantly speeds up numerical experiments due to its higher efficiency on a large-scale multiprocessor computer.

Molecular dynamics simulations of the wild-type and mutated Cyt1A were carried out in parallel scripts with the same strategies, as described in Materials and methods. The initial structures of the wild-type and mutated (K225A) molecules (Fig. 4) exhibited little difference in terms of energy or conformation. The only immediate, and obvious, consequence of replacing K225 with alanine was the loss of the putative hydrogen bonds between the K225 and V1265, L123, and Y189, which hold the side chain of Lys225 in that particular position (Fig. 5). In this way, K225 and β sheet 7; V126, L123 and α helix C; and Y189 and β sheet 6 are locked together, which stabilizes the toxin in terms of domain motion. This is seen in normal mode 8 (frequency 9.72 cm^{-1}). Because the wild type and the mutants K225A, K118A, K198A behaved differently in the interval 1 to 3 ns, we limited our analysis to the first 2 ns. The difference in conformations expressed as the root-mean-square deviation (RMSD) increased from 0.0 for the initial structures to 3.64 after 2 ns of MD. These data thus suggest a progression of significant conformational changes. To separate the effect of the relatively loose N- and C-terminal coils, we

Table 2
RMSD values of average conformations of Cyt1A and its mutants against the initial model conformation (homology modeling from Cyt2Aa1) and each other.

	Cyt2Aa1	Cyt1A	K118A	K198A	K225A
Cyt2Aa1	0.00	2.77	2.84	2.70	3.82
Cyt1A	2.77	0.00	2.82	2.95	3.31
K118A	2.84	2.82	0.00	2.58	3.52
K198A	2.70	2.95	2.58	0.00	3.94
K225A	3.82	3.31	3.52	3.94	0.00

The average conformations were calculated from sampling of the interval 1 ns to 2 ns of MD.

Table 3
Free energy, enthalpy, and entropy differences of the mutants K225A, K118A, and K198A, calculated with respect to a reference tripeptide AKA.

	$\Delta\Delta A$ (kcal/mol)	$\Delta\Delta H$ (kcal/mol)	$\Delta\Delta S$ (cal/(mol K))
K225A	28	86	0.20
K118A	16	59	0.15
K198A	23	20	−0.01

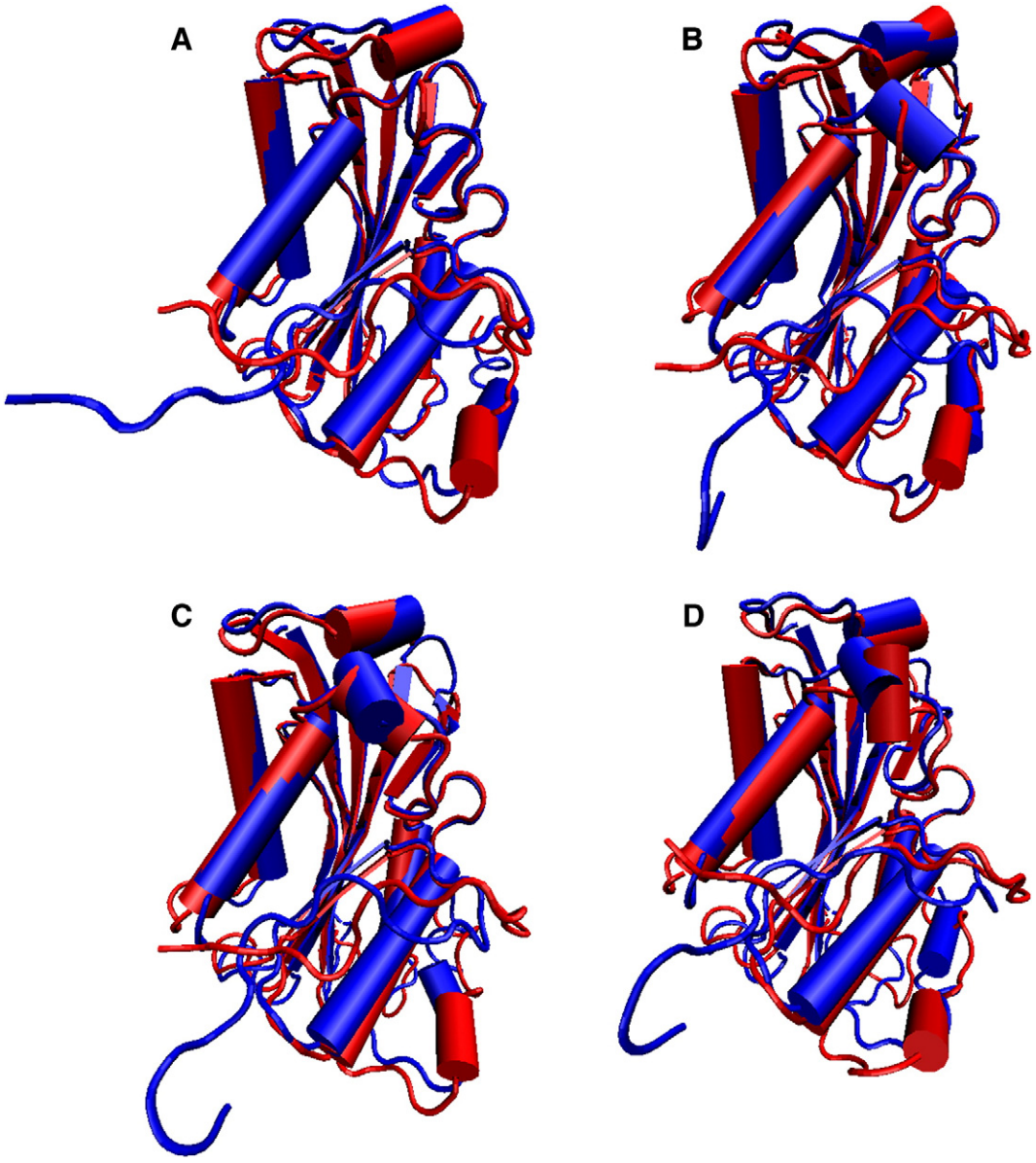

Fig. 4. Superimposed average conformations of Cyt1A and the mutant K225A during molecular dynamics. The average conformations were calculated at 0.5 ns (A), 1.0 ns (B), 1.5 ns (C), and 2.0 ns (D). The wild-type Cyt1A is in red (or a lighter shade of grey in the printed version); the K225A mutant is in blue (dark grey in the printed version).

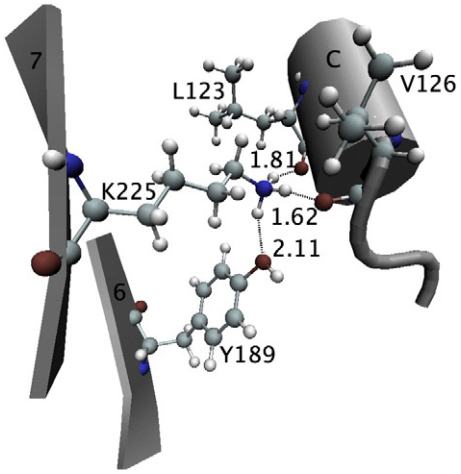

Fig. 5. The hydrogen bonds between K225 and V126, L123, and Y189 with O…H distances shown in angstroms.

excluded residues 1–49 and 241–249 from the calculations, but the RMSD of the average conformations still remained high (2.46) at 2 ns. The average conformations of Cty1A and the K225A mutant at different times are superimposed in Fig. 4. All four α helices of the mutant K225A exhibited significant shift from the wild-type orientation. In the mutant, α helix E moved away from the body of the protein. At 0.5 ns, the end of β sheet 3 became fragmented and β sheet 7 was significantly shortened. At 1.0 ns, changes extended to a new α helix being formed in the loop between α helix D and β sheet 4. Interestingly, at 1.5 ns a new α helix appeared in the wild-type toxin as well, but in a different orientation than in the mutant. At 2.0 ns, β sheet 4 completely unfolded in the mutant, and β sheet 7 in native Cyt1A also shortened. In order to draw a more general conclusion, we computed average conformations of both the native Cyt1A and the K225A mutant from the whole 2 ns simulation; they are superimposed in Fig. 6A. To display the difference more clearly, a colored scale (RMSD from 0 to 2.5, blue–green–red) was employed and the results are shown in Fig. 6B. We can see that all four α helices shifted in the mutant. The β sheet 7 in the mutant toxin was shortened and fragmented. The short β strand 4 underwent changes, mainly in its C-

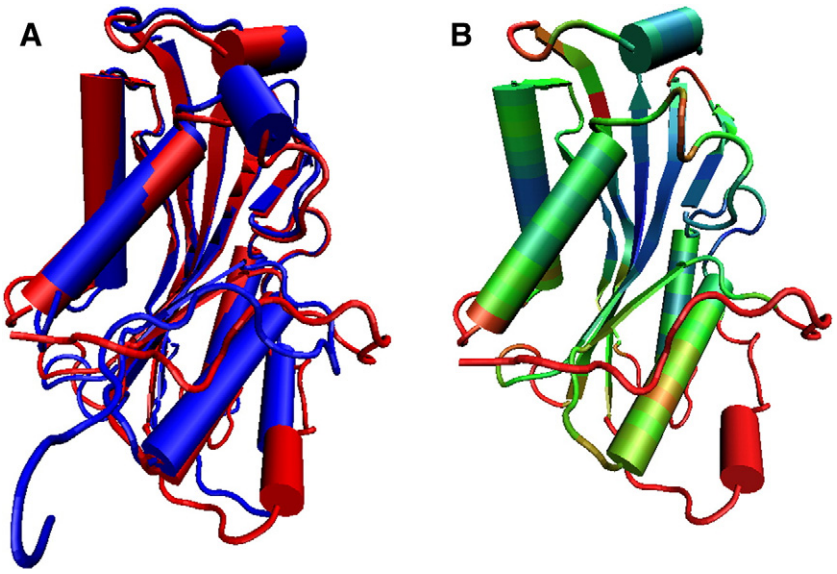

Fig. 6. Superimposed average conformations of the wild-type and mutated toxin molecules at first 2.0 ns of molecular dynamics simulation. (A) The conformation in red color is Cyt1A and the conformation of mutant K225A is in blue. (B) The RMSD differences are shown in RGB color scale (blue 0 to red 2.5).

terminal half. All the loops assumed different conformations in the mutated toxin. Perhaps most significantly, a new α helix F formed in the loop between α helix D and β sheet 4. Two more alternative runs of MD for 2 ns yielded qualitatively similar results. The detected conformation changes indicate that the effects of the single-point mutation K225A are not limited to the immediate vicinity of the residue 225, but with increasing simulation time they spread to other parts of the molecule. The altered conformation may hinder proper binding to the lipid membrane.

We also performed MD simulations with mutations K118A (at the beginning of β sheet 5) and K198A (at the middle of α helix C), which were shown by Ward et al. [14] to retain toxicity in vivo. In contrast with the inactive mutant K225A, MD behavior of these molecules was very similar to that of the wild-type Cyt1A (Fig. 7), and it included hydrogen bond formation between K225, K118, and K198 and their neighboring atoms. Notable differences between K225 and the other two lysines are that the former is in the interior of the protein and mediates interaction between three secondary-structure elements,

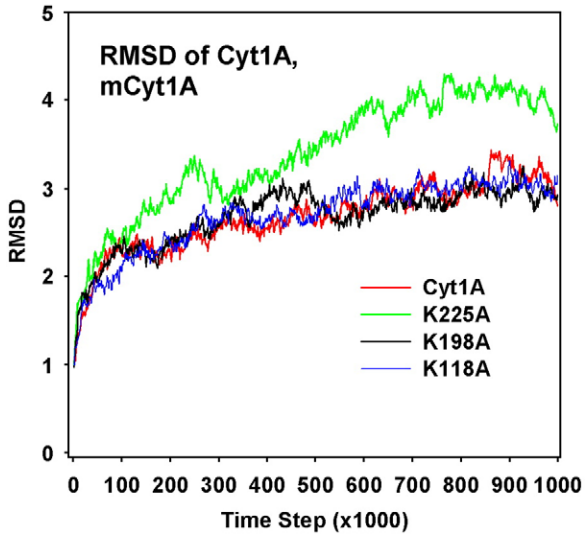

Fig. 7. RMSD values of Cyt1A and the mutants K225A, K118A, and K198A. The values were calculated with respect to the original conformation of Cyt1A as a reference.

while the latter are on the surface and connect only two secondary-structure elements. It is reasonable to expect that these distinctions have functional significance.

4. Conclusions

In order to validate the molecular dynamics model of the solution structure of the toxin Cyt1A, we used resonance energy transfer to measure the distance between the cysteine C190 and the two tryptophans, W158 and W161. With some caveats, the experimental value agreed well with the predicted one. The computer model was used to study the significance of the four blocks of amino-acid residues that are conserved throughout the Cyt toxin family. Our results indicate that the blocks are important for proper folding and stability of the molecule in solution. In MD simulations, an inactive toxin with a single-point mutation exhibited a different behavior from that of the wild-type toxin, with overall changes spread throughout the molecule. This leads to the suggestion that the mutant has lost its activity due to an overall destabilization of the native structure in solution. In contrast, two other single-point mutations, which did not affect Cyt1A's toxicity in the experiments, exhibited MD structures that did not significantly differ from that of the wild-type toxin. Free-energy calculations showed that the mutant K225A is the least stable molecule from amongst the wild-type Cyt1A and two mutants that retained toxicity. The normal mode analysis demonstrated that the side chain of K225 acts as a connector between α helix C and β strands 6 and 7 via three hydrogen bonds, which may be important for the toxin's activity, or at least for its proper conformation in solution.

Acknowledgments

This work was supported by an NSF grant DMS-0241236 and, in part, by the National Research Initiative of the USDA Cooperative State Research, Education and Extension Service, grant 2006-35607-16704/05003. Authors thank Jun Xie of the University of Wisconsin-Milwaukee for technical help in the beginning of the project.

Appendix A. Supplementary data

Supplementary data associated with this article can be found, in the online version, at doi:10.1016/j.bpc.2009.06.005.

References

[1] E. Schnepf, N. Crickmore, J.V. Rie, D. Lereclus, J. Baum, J. Feitelson, D.R. Zeigler, D.H. Dean, *Bacillus thuringiensis* and its pesticidal crystal proteins, Microbiol. Mol. Biol. Rev. 62 (1998) 775–806.

[2] F.A. Drobniewski, D.J. Ellar, Toxin-membrane interactions of *Bacillus thuringiensis* delta-endotoxin, Biochem. Soc. Trans. 16 (1988) 38–40.

[3] M.Z. Haider, D.J. Ellar, Mechanism of action of *Bacillus thuringiensis* insecticidal delta-endotoxin: interaction with phospholipid vesicles, Biochim. Biophys. Acta 978 (1989) 216–222.

[4] B.H. Knowles, M.R. Blatt, M. Tester, J.M. Hornell, J. Carroll, G. Menestrina, D.J. Ellar, A cytolytic delta-endotoxin from *Bacillus thuringiensis* var. *israelensis* forms cation-selective channels in planar lipid bilayers, FEBS Lett. 244 (1989) 259–262.

[5] B. Promdonkoy, D.J. Ellar, Membrane pore architecture of a cytolytic toxin from *Bacillus thuringiensis*, Biochem. J. 350 (2000) 275–282.

[6] S.D. Manceva, M. Pusztai-Carey, P.S. Russo, P. Butko, A detergent-like mechanism of action of the cytolytic toxin cyt1a from *Bacillus thuringiensis* var. *israelensis*, Biochemistry 44 (2004) 589–597.

[7] D.J. Ellar, The insecticidal proteins of *Bacillus thuringiensis*, BT100: Proceedings of a Centennial Symposium Commemorating Ishikawa's Discovery of *Bacillus thuringiensis*, Kurume, Japan, 2001.

[8] P. Butko, F. Huang, M. Pusztai-Carey, W.K. Surewicz, Interaction of the delta-endotoxin CytA from *Bacillus thuringiensis* var. *israelensis* with lipid membranes, Biochemistry 36 (1997) 12862–12868.

[9] P. Butko, Cytolytic toxin Cyt1A and its mechanism of membrane damage: data and hypotheses, Appl. Environ. Microbiol. 69 (2003) 2415–2422.

[10] R. Schleif, Modeling and studying proteins with molecular dynamics, Methods Enzymol. 383 (2004) 28–47.

[11] A.R. Leach, Molecular Modeling: Principles and Applications, Prentice Hall, New York, NY, 2001.

[12] J. Xie, P. Butko, D. Xie, Molecular dynamics simulation of the cytolytic toxin Cyt1A in solution, IEEE Trans. Nanobiosci. 4 (2005) 235–240.

[13] J. Li, P.A. Koni, D.J. Ellar, Structure of the mosquitocidal delta-endotoxin cytb from *Bacillus thuringiensis* sp. *kyushuensis* and implications for membrane pore formation, J. Mol. Biol. 257 (1996) 129–152.

[14] E.S. Ward, D.J. Ellar, C.N. Chilcott, Single amino acid changes in the *Bacillus thuringiensis* var. *israelensis* delta-endotoxin affect the toxicity and expression of the protein, J. Mol. Biol. 202 (1988) 527–535.

[15] W. Humphrey, A. Dalke, K. Schulten, VMD — visual molecular dynamics, J. Mol. Graph. 14 (1996) 33–38.

[16] B.R. Brooks, R.E. Bruccoleri, B.D. Olafson, D.J. States, S. Swaminathan, M. Karplus, CHARMM: a program for macromolecular energy, minimization, and dynamics calculations, J. Comput. Chem. 4 (1983) 187–217.

[17] A.D. MacKerell Jr., B.R. Brooks, C.L. Brooks III, L. Nilsson, Y. Won, M. Karplus, CHARMM: the energy function and its parameterization with an overview of the program, in: P. von Rague Schleyer (Ed.), The Encyclopedia of Computational Chemistry, John Wiley & Sons, New York, NY, 1998.

[18] L. Kale, R. Skeel, M. Bhandarkar, R. Brunner, A. Gursoy, N. Krawetz, J. Phillips, A. Shinozaki, K. Varadarajan, K. Schulten, Namd2: greater scalability for parallel molecular dynamics, J. Comput. Phys. 151 (1999) 283–312.

[19] J.C. Phillips, R. Braun, W. Wang, J. Gumbart, E. Tajkhorshid, E. Villa, C. Chipot, R.D. Skeel, L. Kale, K. Schulten, Scalable molecular dynamics with NAMD, J. Comput. Chem. 26 (2005) 1781–1802.

[20] W. Im, M. Feig, C.L. Brooks III, An implicit membrane generalized Born Theory for the study of structure, stability, and interactions of membrane proteins, Biophys. J. 85 (2003) 2900–2918.

[21] W. Im, M.S. Lee, C.L. Brooks III, Generalized Born Model with a simple smoothing function, J. Comput. Chem. 24 (2003) 1691–1702.

[22] S.H. Fleischman, C.L. Brooks III, Thermodynamics of aqueous solvation: solution properties of alchohols and alkanes, J. Chem. Phys. 85 (2003) 3029.

[23] P. Kollman, Free energy calculations: applications to chemical and biochemical phenomena, Chem. Rev. 93 (1993) 2395–2417.

[24] M. Mezei, D.L. Beveridge, Free energy simulations, Ann. N.Y. Acad. Sci. 482 (1986) 1–23.

[25] T.P. Straatsma, Free Energy Evaluation by Molecular Dynamics Simulations, University of Groningen, Netherlands, 1987.

[26] W.L. Jorgensen, J. Chandrasekhar, J.D. Madura, R.W. Impey, M.L. Klein, Comparison of simple potential functions for simulating liquid water, J. Chem. Phys. 79 (1983) 926–935.

[27] M.P. Allen, D.J. Tildesley, Computer Simulation of Liquids, Clarendon Press, Oxford, 1987.

[28] D. Barash, L.J. Yang, X.L. Qian, T. Schlick, Inherent speedup limitations in multiple time step/Particle Mesh Ewald algorithms, J. Comput. Chem. 24 (2003) 77–88.

[29] P. Butko, F. Huang, M. Pusztai-Carey, W.K. Surewicz, Membrane permeabilization induced by cytolytic delta-endotoxin Cyt1A from *Bacillus thuringiensis* var. *israelensis*, Biochemistry 35 (1996) 11355–11360.

[30] J.M. Schneider, C.I. Barrett, S.S. York, lac repressor cysteine-140 reacts selectively with a fluorescent probe bound to the core–headpiece interface, Biochemistry 23 (1984) 2221–2226.

[31] J.R. Lakowicz, Principles of Fluorescence Spectroscopy, Springer, New York, NY, 2006.

[32] B.W. van der Meer, G. Coker, S.Y.S. Chen, Resonance Energy Transfer: Theory and Data, VCH Publishers, New York, NY, 1994.

[33] B. Corry, D. Jayatilaka, P. Rigby, A flexible approach to the calculation of resonance energy transfer efficiency between multiple donors and acceptors in complex geometries, Biophys. J. 89 (2005) 3822–3836.

[34] N. Guex, M.C. Peitsch, Swiss-model and the Swiss-PdbViewer: an environment for comparative protein modeling, Electrophoresis 18 (1997) 2714–2723.

[35] D. Frishman, P. Argos, Knowledge-based secondary structure assignment, Proteins Structure Function Genetics 23 (1995) 566–579.